High-Pressure Naphthalene–Xenon Phase Behavior

Mark A. McHugh,* James J. Watkins, and Brian T. Doyle
Department of Chemical Engineering, The Johns Hopkins University, Baltimore, Maryland 21218

Val J. Krukonis
Phasex Corporation, 360 Merrimack Street, Lawrence, Massachusetts 01843

The high-pressure phase behavior of the naphthalene–xenon system is experimentally determined. Naphthalene solubility isotherms are obtained at 34.9, 40.0, and 45.0 °C over a range of pressures from 105 to 270 bar. The pressure–temperature projection of the solid–liquid–gas (SLG) line is obtained, and the upper critical end point (UCEP) is found at 46.4 °C, 136.8 bar, and a naphthalene mole fraction of 0.135. The location of the UCEP differs from a previously determined value; this discrepancy is attributed to differences in the experimental techniques used to obtained the UCEP. The phase diagram for the naphthalene–xenon system can be generated by using the Peng–Robinson and the Sanchez–Lacombe equations of state each with two mixture parameters fit to the SLG line. Although both equations represent the data with about the same accuracy, the Sanchez–Lacombe equation does a better job fitting the SLG line and the observed liquid–gas and solid–gas phase inversions.

In a previous paper (Krukonis et al., 1984), we reported on the solubilities of naphthalene in supercritical xenon (T_C = 16.7 °C, P_C = 58.8 bar) at temperatures of 34.9, 39.8, and 45.0 °C and for pressures to 225 bar. We also presented preliminary data on the pressure–temperature (P–T) trace of the xenon–naphthalene, solid–liquid–gas (SLG) line. The results from that earlier study show that supercritical xenon has a solvent power which is comparable to that of supercritical carbon dioxide, ethylene, and ethane. Other investigators have also corroborated this finding.

Smith et al. (1987), who characterize the solvent power of a supercritical fluid based on the π^* polarity/polarizability scale established by Kamlet, Taft, and co-workers, find that xenon has a solvent power that is better than that of supercritical sulfur hexafluoride, is comparable to that of supercritical ethane, but is not as good as that of supercritical carbon dioxide or ammonia. French and Novotony (1986) used xenon as the mobile phase for supercritical fluid chromatography/FTIR spectrometry investigations. They were able to solubilize heavy phenols and aldehydes in supercritical xenon. It should be noted that, although liquid xenon is also a good solvent (Everett and Stageman, 1978; Marshall et al., 1983; Rentzepis and Douglas, 1981), supercritical xenon exhibits much greater solvent capacity.

In the present work, we add to our previously reported solubility isotherms (34.9, 39.8, and 45.0 °C), we also extend the SLG line to the upper critical end point (UCEP), and we measure the portion of the critical-mixture curve which intersects the UCEP. Figure 1 shows schematically the type of P–T behavior expected for binary mixtures of naphthalene, a heavy, nonvolatile solid, and supercritical xenon (Krukonis et al., 1984). The characteristics of this class of phase behavior are that the critical temperature of the fluid (T_{C1}) is much lower than the normal melting temperature of the solid (T_{M2}), the critical conditions of the two components differ substantially, and the molecular size, shape, structure, and intermolecular potential of the two components are also usually very different. As shown in Figure 1, the critical-mixture (L = G) curve is intersected by the SLG line in two locations: the UCEP and the LCEP (i.e., the lower critical end point). Supercritical fluid extraction of a solid occurs in the P–T region between the two branches of the SLG line, since only solid–fluid behavior is observed in this region regardless of the system pressure.

One objective of this study was to obtain the entire SLG line starting at the normal melting point of naphthalene (T_{M2} = 80.2 °C) and ending at the UCEP. Care was taken in determining the location of the UCEP since various types of phase transitions can occur near the SLG line depending on the overall composition of the mixture (van Welie and Diepen, 1961a). These phase transitions are described in detail in the following section of this paper. At the UCEP, a vapor–liquid critical point occurs in the presence of excess solid, and critical opalescence can be observed—naphthalene–xenon mixtures appear reddish orange. To further verify the location of the UCEP, we measured the portion of the critical-mixture curve which intersects the SLG line. The critical-mixture curve represents liquid + vapor critical points for mixtures with varying concentrations of naphthalene and xenon. Once the SLG line was determined, more solid-solubility data were obtained at 34.9, 39.8, and 45.0 °C. The other objective of this study was to show how the resultant phase behavior can be represented by the Peng–Robinson equation of state and the Sanchez–Lacombe equation of state. The merits of each of these approaches are discussed.

Experimental Section

The experimental apparatus used in this study is described in detail elsewhere (McHugh et al., 1984a). A schematic diagram of the experimental apparatus is shown in Figure 2. The main component of the system is a high-pressure, variable-volume view cell. Xenon is quantitatively transferred into the high-pressure view cell which has been previously charged with a measured amount of naphthalene. The naphthalene–xenon mixture, viewed through a boroscope (Olympus, Model D100-048-000-90) placed against a Pyrex window secured at one end of the cell, is mixed by a glass-encased stirring bar activated by a magnet located below the cell. The contents of the cell can also be projected onto a video monitor (Panasonic, Model BT-S1900N) using a video camera (Panasonic, Model WV-3240) linked to the boroscope. The advantage of using the video equipment is that the image of the cell contents is enlarged several times and, hence, is easier to analyze and interpret.

In contrast to the first-melting technique that was used previously to determine the P–T trace of the SLG line

* Author to whom correspondence should be addressed.

0888-5885/88/2627-1025$01.50/0

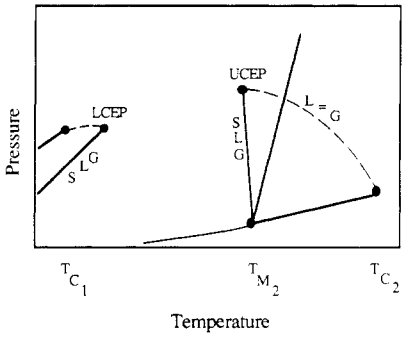

Figure 1. Schematic pressure–temperature (P–T) diagram for a mixture consisting of a heavy, nonvolatile solid and a light gas.

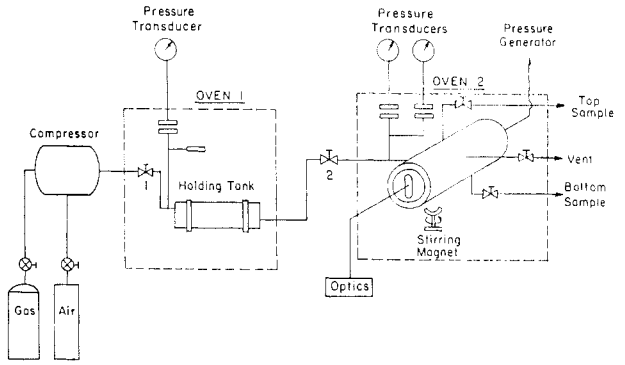

Figure 2. Schematic diagram of the experimental apparatus used in this study.

(Krukonis et al., 1984), we determine the P–T trace of the SLG line and the location of the UCEP using a more exacting technique (van Welie and Diepen, 1961a). After a known amount of naphthalene and xenon is loaded in the view cell, the mixture is compressed to a high pressure by a movable piston fitted within the cell and is heated until either two phases, liquid + vapor, or a single phase, liquid, vapor, or fluid, exists in the cell. The type of single phase can only be determined by crossing a phase boundary. The high-pressure view cell is isobarically cooled very slowly, and the type of phase transition is noted. Four different types of transitions can be observed depending on the overall mixture composition.

If a liquid and a vapor are initially present, and if, upon isobaric cooling, a solid falls out of solution, an SLG point is obtained. However, if all of the liquid in the cell disappears before solid is formed, the transition is a dew point as shown in Figure 3A. If all of the vapor disappears before solid is formed, the transition is a bubble point as shown in Figure 3B. Notice that a critical point does not occur for the constant-composition, P–T loop shown in Figure 3A, because the loop is intersected by a solid-phase region. But, a critical point does occur on the P–T loop for the mixture shown in Figure 3B.

Finally, if only a single vapor or liquid phase is initially present in the cell, and if, upon isobaric cooling, solid precipitates from the solution without the formation of a third phase, the temperature of the solid–fluid transition can be either less than (Figure 3A) or greater than (Figure 3B) the SLG temperature. By use of the technique described in the previous paragraphs, the solubility of naphthalene in supercritical xenon at the UCEP is obtained by repeating the SLG determination with differing overall mixture compositions.

The critical-mixture curve is measured in the following manner (Occhiogrosso et al., 1986). At a temperature slightly higher than the UCEP temperature, a vapor–liquid mixture at a fixed overall concentration is compressed to

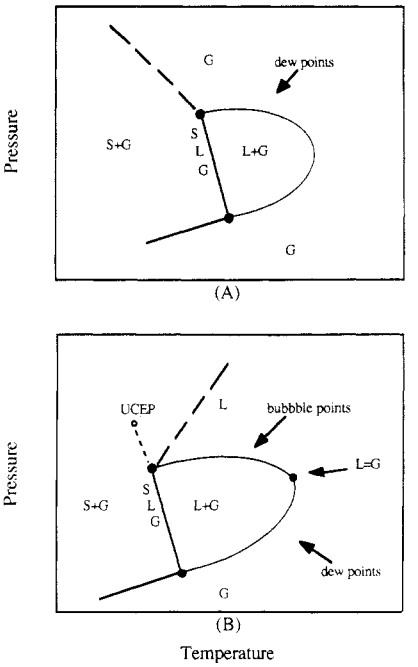

Figure 3. Schematic P–T diagram showing the effect of composition on the types of phase transitions which can occur near the upper critical end point (UCEP). Part A shows the solid–liquid–gas (SLG) line with a section of a constant-composition loop at a concentration of heavy component which is less than that at the UCEP. Part B shows the SLG line with a section of a constant-composition loop at a concentration of heavy component which is greater than that at the UCEP. The dotted portion of the SLG line leading to the UCEP is not observable since the concentration is too high.

Table I. Pressure–Temperature Trace of the Solid–Liquid–Gas Line for the Naphthalene–Xenon System Obtained in This Study

P, bar	T, °C	P, bar	T, °C
136.8	46.43[a]	108.2	47.44
136.5	46.59	108.2	47.81
136.1	46.43	102.8	47.34
135.4	46.72	102.8	47.96
131.2	46.35	100.1	48.00
129.8	46.39	96.5	48.10
126.4	46.13	94.1	48.10
124.1	46.69	88.3	49.00
113.4	47.10	79.8	51.50
		48.3	63.20

[a] UCEP, 13.5 mol % naphthalene.

a single phase. The pressure is then isothermally decreased very slowly until the system becomes turbid and a second phase just begins to precipitate. The transition is a critical-mixture point if critical opalescence is observed during the transition process and if two phases of equal volume are present when the mixture phase separates.

The reported pressures, measured with a bourdon-tube Heise gauge, are accurate to within ±0.34 bar, and the reported temperatures, measured with a platinum RTD (Degussa Company, calibrated on the 1968 IPTS scale), are accurate to within ±0.1 °C. The reported solid-solubility and critical-mixture data have an estimated, accumulated error which is less than 2.0% of the absolute value. The naphthalene, obtained from Fischer Scientific (spectroscopic grade), was used without further purification, and the xenon, donated by BOAC group, was also used without further purification.

Results and Discussion

The P–T behavior of the naphthalene–xenon system is shown in Figure 4 and is listed in Tables I and II. The

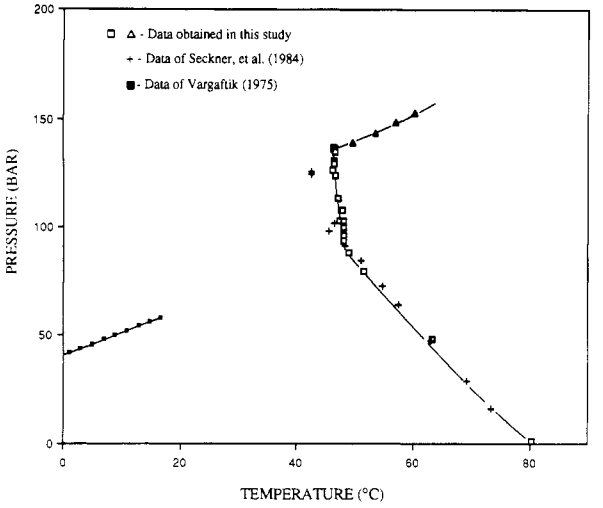

Figure 4. Experimentally determined pressure–temperature diagram for the naphthalene–xenon system obtained in this study.

Table II. Pressure–Temperature–Concentration Data for the Section of the Critical-Mixture Curve Which Intersects the UCEP

P, bar	*T*, °C	mol % naphthalene
139.2	49.6	13.48
144.1	53.6	13.48
148.8	57.1	13.48
152.9	60.2	13.48

P–T trace of the SLG line and the critical-mixture curve is determined within ±0.1 °C and 0.5 bar. As shown in Table II, the concentration of naphthalene in supercritical xenon remains essentially constant along the section of the critical-mixture curve near the UCEP. This behavior has been observed for other naphthalene–supercritical fluid systems (van Hest and Diepen, 1960; van Welie and Diepen, 1961b, 1963).

The UCEP for the naphthalene–xenon system is 46.4 ± 0.1 °C, 136.8 ± 0.5 bar, and 13.5 ± 0.1 mol % naphthalene. The location of the UCEP is determined as the intersection of the SLG line with the critical-mixture curve. The low-pressure SLG data obtained by Krukonis et al. (1984) are in good agreement with the data obtained in this study. However, at high pressures near the UCEP, the first-melting technique used by Krukonis et al. leads to spurious results as shown in Figure 4.

Also shown in Figure 4 is the vapor-pressure curve for pure xenon (Vargaftik, 1975), which should be very close to the branch of the SLG line which ends at the LCEP (McHugh et al., 1984a,b; van Gunst et al., 1953). The location of the LCEP, which is dependent on the solubility level of naphthalene in xenon, is expected to be very close to the critical point of pure xenon since the solubility of a heavy solid in a supercritical fluid near its critical point is usually quite low (McHugh and Krukonis, 1986).

The shape of the SLG line results from a compromise between the effect of hydrostatic pressure on the melting point of pure naphthalene, the solubility of xenon in the naphthalene-rich liquid phase, and the solubility of naphthalene in the xenon-rich gas phase (Paulaitis et al., 1983). As seen in Figure 4, the initial slope of the SLG line, starting at the melting point of naphthalene, is reasonably linear between 80 °C and 1 bar and 50 °C and 87 bar. For this section of the SLG line, the solubility of naphthalene in the xenon-rich gas phase is expected to be extremely low. Since the initial slope of the SLG line is negative, the hydrostatic-pressure effect is dominated by the solubility of xenon in the naphthalene-rich liquid phase along this portion of the line. The higher the solubility, the larger the melting point depression of naphthalene. Assuming that naphthalene and xenon form an ideal liquid solution, the solubility of xenon in liquid naphthalene can be estimated by using the following expression (De Swaan Arons and Diepen, 1963)

$$\ln x_{Xe} = -\frac{\Delta H^F}{R}\left\{\frac{1}{T} - \frac{1}{T_{M2}}\right\} + \frac{P\Delta v}{RT} \qquad (1)$$

where T_{M2} represents the normal melting temperature of naphthalene (80.2 °C), Δv represents the difference between the volume of pure, solid naphthalene and pure subcooled liquid naphthalene (−18.7 cm^3/mol (De Swaan Arons and Diepen, 1963)), ΔH^F is the heat of fusion of naphthalene (4540 cal/mol (De Swaan Arons and Diepen, 1963)), and R is the gas constant. Using eq 1 with *P–T* data from the initial slopes of their respective SLG lines, it can easily be shown that xenon is more soluble in liquid naphthalene than ethane (van Welie and Diepen, 1963), ethylene (van Gunst et al., 1953), carbon dioxide (McHugh and Yogan, 1984), and methane (van Hest and Diepen, 1960). It also follows that the melting point depression of naphthalene caused by xenon, 34 °C, is greater than that caused by ethane, 25 °C, ethylene, 29 °C, carbon dioxide, 20 °C, and methane, 5 °C.

At pressures greater than 87 bar, the solubility of xenon in the naphthalene-rich liquid phase does not increase very rapidly, and hence, the shape of the SLG line is a result of a compromise between the effect of hydrostatic pressure, which imparts a positive slope to the line, and the solubility of naphthalene in supercritical xenon, which determines the location of the UCEP. If the solubility of naphthalene in supercritical xenon is moderately high, the UCEP will occur at modest pressures very soon after the linear region of the SLG line similar to what occurs with the naphthalene–ethylene and naphthalene–ethane systems. However, if the solubility of naphthalene is low, the UCEP does not occur until very high pressures as with the naphthalene–methane system, or it does not occur at all as with the helium–hydrogen system (Streett, 1973).

A number of interesting phase inversions occur with the naphthalene–xenon system. At pressures above about 80 bar, the density of the naphthalene-rich liquid phase and the xenon-rich gas phase along the SLG line becomes greater than that of the pure, solid naphthalene phase. Hence, solid naphthalene floats to the top of the view cell. This behavior is quite interesting since the xenon-rich gas phase is virutally pure xenon at these conditions and it is somewhat unexpected that the gas phase would become more dense than the solid phase. The solid–gas inversion probably occurs because xenon is one of the more dense supercritical fluids and it is very compressible. It is perhaps more unexpected that the addition of supercritical xenon to liquid naphthalene would raise the density of the resultant liquid mixture above that of the solid since usually the addition of a gas to a liquid decreases the density. However, as stated before, xenon is a very dense gas which also has a molecular weight that is close to that of naphthalene. It is conjectured that the solid–liquid inversion occurs because the partial molar volumes of xenon and naphthalene in the liquid phase are probably less than their respective molar volumes at the same temperature and pressure.

If the pressure is increased to about 112 bar, the xenon-rich gas phase becomes more dense than the liquid phase, and therefore, the gas phase settles to the bottom of the cell with the liquid phase in the middle and the solid phase at the top. The liquid–gas density inversion is also

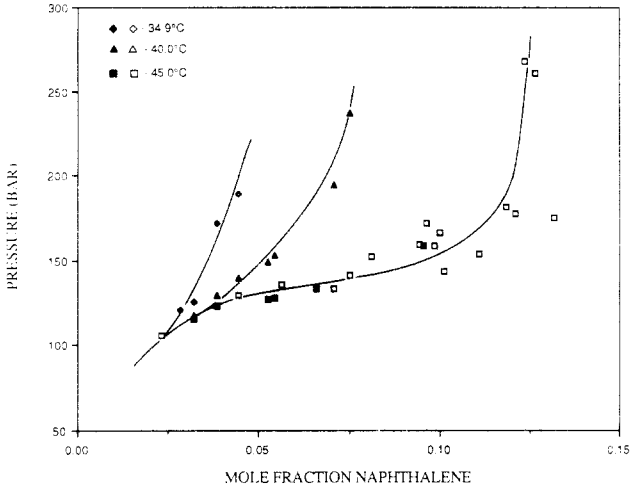

Figure 5. Comparison of the solid-solubility data obtained in this study (open symbols) with the data of Krukonis et al. (1984) (closed symbols).

observed in the L + G region of the phase diagram at pressures greater than 112 bar. At 80 bar, the gas phase is probably greater than 99 mol % xenon, while at 112 bar it has probably only been reduced to 98 mol %. Since the solubility of naphthalene in the gas phase increases by only a small amount and since the operating condition is far from the critical point of pure xenon, it seems unlikely that the inversion is driven by a partial molar volume phenomenon. The liquid–gas inversion is probably a density- or pressure-driven phenomenon—that is, the gas phase is still highly compressible, and thus, the density increases by a significant amount as the pressure is increased. At the same time, the concentration of the liquid phase has not changed considerably and the liquid is not expected to be very compressible. Therefore, the density of the liquid should remain virtually unchanged as the pressure is increased. Phase inversions have been observed in other solute–supercritical fluid systems (McHugh and Yogan, 1984), and thus, it is very important from a processing standpoint to be cognizant that these inversions can occur.

Listed in Table III and shown in Figure 5 are the naphthalene–xenon solubility isotherms at 34.9, 40.0, and 45.0 °C. At 34.9 °C the solubility of naphthalene in supercritical xenon quickly reaches a limiting value of about 4.5 mol % at 200 bar. If the temperature is increased to 40.0 °C, the limiting solubility reaches about 7.5 mol % at 245 bar. However, if the temperature is raised 5 more deg to 45.0 °C, the solubility isotherm shows an inflection at about 135 bar where the solubility increases quite significantly for a small change in pressure. The inflection in the solubility curve at 45.0 °C and 135 bar is caused by the vapor–liquid critical point which occurs at the UCEP. The scatter in the data for this isotherm is expected since the solvent power of a supercritical fluid is very sensitive to small changes in pressure and temeprature near a critical-mixture point (McHugh and Krukonis, 1986). Notice, also, that at 45.0 °C the solubility of naphthalene in supercritical xenon continues to increase to values as high as 13 mol % as the pressure is increased above 135 bar. Eventually a limiting solubility is reached at sufficiently high-enough pressures.

Data Reduction

The phase-equilibrium data obtained in this study are modeled with the Peng–Robinson equation of state (Peng and Robinson, 1976) and the Sanchez–Lacombe equation of state (Sanchez and Lacombe, 1978). The Peng–Robinson equation is a cubic equation which uses a van der Waals type repulsive term with a modification of the van der Waals attractive term, while the Sanchez-Lacombe equation is a lattice-gas equation which uses a van der Waals attractive term with a lattice-gas repulsive term. Our objectives in this section are to show the merits of each of these equations for calculating high-pressure phase behavior and to describe how the phase diagram for solid–gas systems can be readily calculated by fitting the parameters of the equation of state to the P–T trace of the SLG line (McHugh et al., 1984a,b). A detailed development of the necessary equations for modeling the SLG line is found elsewhere (McHugh and Krukonis, 1986) and is, therefore, only briefly described here.

Table III. Solubility of Naphthalene in Supercritical Xenon Obtained in This Study

P, bar	naphthalene, mol %	P, bar	naphthalene, mol %
T = 34.9 °C			
189.1	4.53		
T = 40.0 °C			
237.4	7.52		
139.7	4.53		
194.8	7.24		
T = 45.0 °C			
105.5	2.36	159.6	9.64
129.4	4.53	166.1	10.22
133.0	7.24	171.6	9.84
135.9	5.76	175.2	13.48
141.2	7.69	177.7	12.34
143.2	10.33	181.1	12.09
152.3	8.30	260.3	12.91
153.6	11.32	268.0	12.60
158.7	10.07		

At equilibrium, the fugacities of each of the components present in each of the phases must be equal. Although there are four fugacity equalities along the SLG line, one of the equations is redundant. We chose to solve the following three equations:

$$F_2^G = F_2^S \tag{2}$$

$$F_2^G = F_2^L \tag{3}$$

$$F_1^G = F_1^L \tag{4}$$

where F represents the fugacity, subscripts 2 and 1 represent naphthalene and xenon, and the superscripts S, L, and G represent the solid, liquid, and gas phases, respectively. Solid naphthalene, with a density of 1.145 g/cm^3, will be considered as a pure solid which is incompressible over the range of pressures of interest in this study (Vaidya and Kennedy, 1971). Therefore, eq 2 becomes

$$y_2\phi_2{}^G P = P_2{}^{sub}\phi_2{}^{sub} \exp\left\{v_2{}^s\left(\frac{P - P_2{}^{sub}}{RT}\right)\right\} \tag{5}$$

where y_2 is the mole fraction of naphthalene, $\phi_2{}^{sub}$ is the fugacity coefficient of naphthalene, P is the system pressure, $P_2{}^{sub}$ is the sublimation pressure of naphthalene, and $v_2{}^s$ is the molar volume of solid naphthalene.

Equations 3 and 4 can be written as

$$y_2\phi_2{}^G = x_2\phi_2{}^L \tag{6}$$

$$y_1\phi_1{}^G = x_1\phi_1{}^L \tag{7}$$

where x represents a liquid-phase mole fraction.

When the Peng–Robinson equation is used to determine

the fugacity coefficients, the following mixing rules are used:

$$a_{mix} = \sum_i \sum_j x_i x_j a_{ij} \quad (8)$$

$$a_{ij} = (a_{ii}a_{jj})^{0.5}(1 - k_{ij}) \quad (9)$$

$$b_{mix} = \sum_i \sum_j x_i x_j b_{ij} \quad (10)$$

$$b_{ij} = 0.5[(b_{ii} + b_{jj})(1 - \eta_{ij})] \quad (11)$$

where k_{ij} and η_{ij} are mixture parameters which are determined by fitting the Peng–Robinson equation to the SLG line and a_{ii} and b_{ii} are pure component parameters as defined by Peng and Robinson (1976). With these mixing rules, the expression for the fugacity coefficient becomes

$$\ln \phi_i = \frac{(b_{mix}N)'}{b_{mix}}(Z - 1) - \ln (Z - B) - \frac{A}{2.828B}\left((2\sum x_j a_{ij})/a - \frac{(b_{mix}N)'}{b_{mix}} \right) \ln \left(\frac{Z + 2.414B}{Z - 0.414B} \right) \quad (12)$$

where Z is the mixture compressibility, N is the total number of moles of the mixture, and A and B are pure component parameters as defined by Peng and Robinson (1976). $(b_{mix}N)'$ is given as

$$(b_{mix}N)' = \partial(b_{mix}N)/\partial N_i = 2\sum_k^N x_k b_{ik} - b_{mix} \quad (13)$$

Equation 13 is the corrected version of eq 5.17d given by McHugh and Krukonis (1986). If η_{ij} is set equal to zero, the mixing rule for b_{mix} and the equation for the fugacity coefficient reduces to the form given by Peng and Robinson (1976). The pure component characteristic properties needed with the Peng–Robinson equation include the critical temperature, the critical pressure, and the accentric factor for each of the components.

The Sanchez–Lacombe equation of state, which is based on lattice-fluid theory, is also used in this study. This equation of state is

$$\tilde{P} = \tilde{T}\left\{ \left(\frac{1}{r} - 1 \right)\tilde{\rho} - \ln (1 - \tilde{\rho}) \right\} - \tilde{\rho}^2 \quad (14)$$

where $\tilde{P}$, $\tilde{T}$, and $\tilde{\rho}$ are the reduced pressure, temperature, and density, respectively. The parameter r represents the number of lattice sites occupied by a molecule and is given by

$$r = \frac{MP^*}{RT^*\rho^*} \quad (15)$$

where M is the molecular weight and R is the gas constant. For xenon, T^*, P^*, and ρ^*, the characteristic temperature, pressure, and close-packed mass density, are obtained by fitting the Sanchez–Lacombe equation to liquid molar volume data at temperatures between 45 and 55 °C and pressures between 80 and 150 bar (Michels et al., 1954) and to the vapor–liquid equilibrium (VLE) line (Vargaftik, 1975) to within 11 °C of the critical temperature. The pressure–temperature conditions chosen for fitting the liquid molar volume data are in the vicinity of the UCEP which is the most important P–T region for this study. The fit to VLE data gives reliable values for T^* and P^*, while the fit to liquid molar volume data provides a reliable value for ρ^*. The pure component parameters for naphthalene are obtained by fitting the Sanchez–Lacombe equation to liquid molar volume data at 80–90 °C and over a pressure range of 100–200 bar (Russell and Hottel, 1938) and to VLE data (API Tables, 1980) in a temperature range of 180–218 °C. The Sanchez–Lacombe equation was also simultaneously fit to the normal melting point for naphthalene when determining the characteristic parameters. If the melting point of naphthalene is neglected when fitting pure component parameters, the calculated melting point for naphthalene could be off by several degrees. The characteristic parameters for xenon and naphthalene are given in Table IV.

For naphthalene–xenon mixtures, the characteristic temperature is defined as

$$T^*_{mix} = \epsilon_{mix}/R \quad (16)$$

where ϵ_{mix}, the interactive energy for the mixture, is expressed as (Sanchez and Lacombe, 1978)

$$\epsilon_{mix} = (1/v^*_{mix})\sum_i \sum_j \phi_i \phi_j \epsilon_{ij} v^*_{ij} \quad (17)$$

$$\epsilon_{ij} = (\epsilon_{ii}\epsilon_{jj})^{0.5}(1 - k_{ij}) \quad (18)$$

The close-packed volume for the mixture, v^*_{mix}, is given as

$$v^*_{mix} = \sum_i \sum_j \phi_i \phi_j v^*_{ij} \quad (19)$$

$$v^*_{ij} = 0.5[(v^*_{ii} + v^*_{jj})(1 - \eta_{ij})] \quad (20)$$

and ϕ_i, the close-packed volume fraction of component i, is defined as

$$\phi_i = \frac{m_i/\rho_i^*}{m_i/\rho_i^* + m_j/\rho_j^*} \quad (21)$$

where m_i is the weight fraction of component i. The mixture parameter, k_{ij}, accounts for deviations of the mixture interaction energy from the geometric mean of the pure component energies, and η_{ij}, a second mixture parameter, accounts for the deviation of the arithmetic average in the close-packed volume of the mixture.

The characteristic pressure of the mixture is given as

$$P^*_{mix} = \frac{RT^*_{mix}}{v^*_{mix}} \quad (22)$$

And the number of lattice sites occupied by an $r$mer in the mixture is given by

$$r = \sum_i x_i r_i^\circ \quad (23)$$

where x_i represents the mole fraction of component i and r_i° represents the number of sites occupied by a molecule in the pure state.

Fugacity coefficients are obtained with the Sanchez–Lacombe equation of state by using the following equation:

$$\ln \left\{ \frac{f_2^G}{Px_2} \right\} = \ln \phi_m - x_1 \{\partial \ln \phi_m/\partial x_1\}_{T,P} \quad (24)$$

The expressions for the fugacity coefficient of the mixture and for the derivative of the fugacity coefficient with respect to composition are given in the Appendix.

The fit of the SLG line using either the Peng–Robinson or the Sanchez–Lacombe equation with a given estimate of k_{ij} and η_{ij} was obtained in the following manner. At a fixed pressure and temperature, eq 5 was solved to determine the composition of naphthalene in the gas phase. Next, eq 6 and 7 were solved by guessing a liquid-phase composition and iterating until the equations were satisfied. The sum of the calculated liquid-phase mole fractions was then checked. If this sum was greater than 1.0, the temperature was adjusted downward slightly and the

Table IV. Characteristic Parameters for Xenon and Naphthalene Used with the Sanchez–Lacombe Equation of State

component	ρ^*, g/cm^3	T^*, K	P^*, bar
xenon	3.040	354	2483
naphthalene	1.109	668	4543

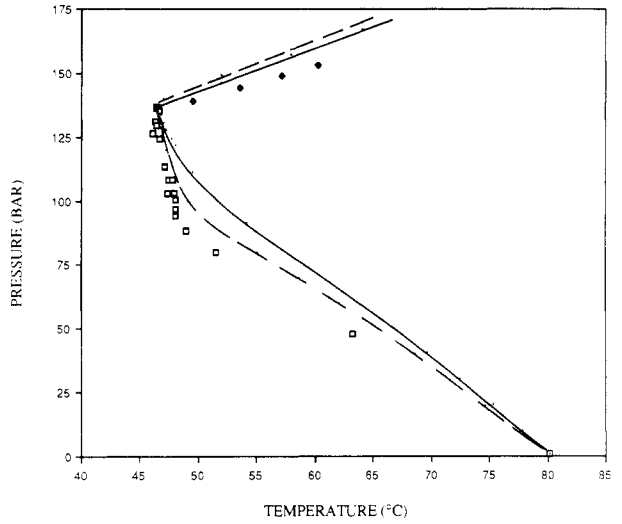

Figure 6. Comparison of calculated and experimental phase behavior. The solid lines are calculations with the Peng–Robinson equation with k_{ij} equal to 0.020 and η_{ij} equal to −0.025. The dashed lines are calculations with the Sanchez–Lacombe equation with k_{ij} equal to 0.030 44 and η_{ij} equal to −0.0354.

calculational procedure was restarted at eq 5 using the same pressure as before. If the sum of the liquid-phase mole fractions is less than 1.0, the temperature is raised slightly and again the calculational procedure is restarted at eq 5 using the same pressure as before. If the sum is equal to 1.0, the result is recorded as a point on the calculated SLG line, the pressure is increased, and the calculations are restarted at eq 5. A vapor–liquid critical point is predicted at the UCEP. Once the SLG curve is fit and the values for k_{ij} and η_{ij} are determined, the critical-mixture curve and the solid-solubility isotherms are calculated. For both the Peng–Robinson and the Sanchez–Lacombe equations, we found that changing k_{ij} had a large effect on the UCEP temperature and a smaller effect on the UCEP pressure, while changing η_{ij} had a large effect on the UCEP pressure and a smaller effect on the UCEP temperature.

Using the Peng–Robinson equation as described in the previous paragraphs, it was not possible to fit the normal melting point of naphthalene to within 2 °C. However, if the value for b_{22} is multiplied by 0.9944, the melting point could be determined within 0.1 °C. This correction factor was used throughout the remainder of the calculations.

The fit of the SLG line and the calculated critical-mixture curve using the Peng–Robinson equation is shown in Figure 6. With a value of 0.020 for k_{ij} and −0.025 for η_{ij}, the calculated UCEP is 46.5 °C and 136.8 bar. As shown in Figure 6, the calculated and experimental UCEP are in good agreement, while the calculated SLG line is in poor agreement with experimental data. A better fit of the low-pressure range of the SLG line can be obtained with different values of k_{ij} and η_{ij}; however, it is not possible to simultaneously fit the entire curve and the UCEP. It was also not possible to obtain as good a fit of the UCEP with η_{ij} set equal to zero. Dieters and Schneider (1976) also found that two mixture parameters are needed with the Redlich–Kwong equation of state to fit high-pressure

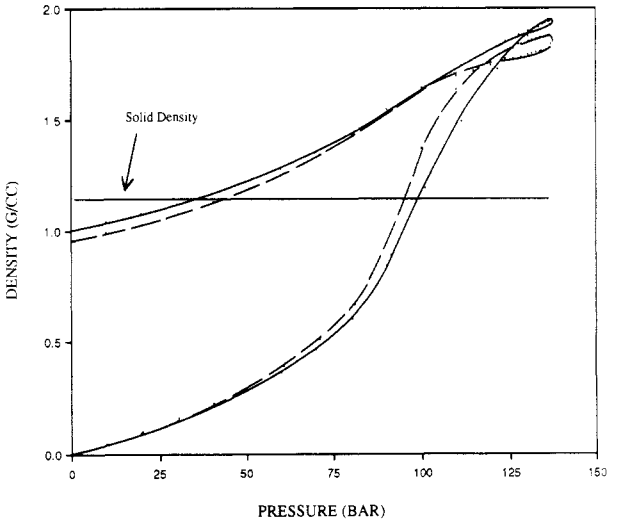

Figure 7. Comparison of calculated and experimental densities along the solid–liquid–vapor line. The solid lines are calculations with the Peng–Robinson equation with k_{ij} equal to 0.020 and η_{ij} equal to −0.025. The dashed lines are calculations with the Sanchez–Lacombe equation with k_{ij} equal to 0.030 44 and η_{ij} equal to −0.0354.

phase behavior data. The calculated pressure projection of the critical-mixture curve, which was determined using the values of k_{ij} and η_{ij} found from the fit of the SLG, is in fair agreement with experimental data as shown in Figure 6. The pressure along the calculated critical-mixture curve is consistently higher than the experimentally observed data.

Figure 7 shows the calculated phase inversions which occur along the SLG line. At pressures greater than 130 bar, the Peng–Robinson equation predicts that the gas phase becomes more dense than the liquid phase. Experimentally the inversion of these phases occurs at about 112 bar. The calculated solid–gas inversion, 100 bar, is also greater than the experimentally observed value of about 80 bar.

Calculated solid–solubility isotherms are shown in Figure 8. In general, the Peng–Robinson equation of state overpredicts the solubility of naphthalene in supercritical xenon by about 10% at 35 °C and by 14–16% at 45 °C and pressures near the UCEP. It is not surprising that the predictions are off by such a large amount near the UCEP since these operating conditions are very close to the vapor–liquid critical point which occurs at the UCEP. If k_{ij} and η_{ij} are allowed to vary slightly, a much better fit of the solubility isotherms could be obtained at the cost of a poorer fit of the SLG line and the UCEP. Nevertheless, by use of mixture parameters fit to the P–T of the SLG line, a reasonable estimate can be made of the solubility of the solid in the supercritical fluid.

The analogous phase equilibrium calculations made with the Sanchez–Lacombe equation of state are also shown in Figures 6–8. With a value of 0.030 44 for k_{ij} and −0.0354 for η_{ij}, the UCEP is calculated as 46.5 °C and 136.9 bar. These values for k_{ij} and η_{ij} are similar to those used with the Peng–Robinson equation. As shown in Figure 6, the fit of the SLG line is much better with the Sanchez–Lacombe equation than with the Peng–Robinson equation. However, the pressure along the critical-mixture curve calculated with the Sanchez–Lacombe equation was greater than that of the data or the values calculated with the Peng–Robinson equation.

Figure 7 shows that the phase inversions along the SLG line calculated with the Sanchez–Lacombe equation were in much better agreement with the experimental data than

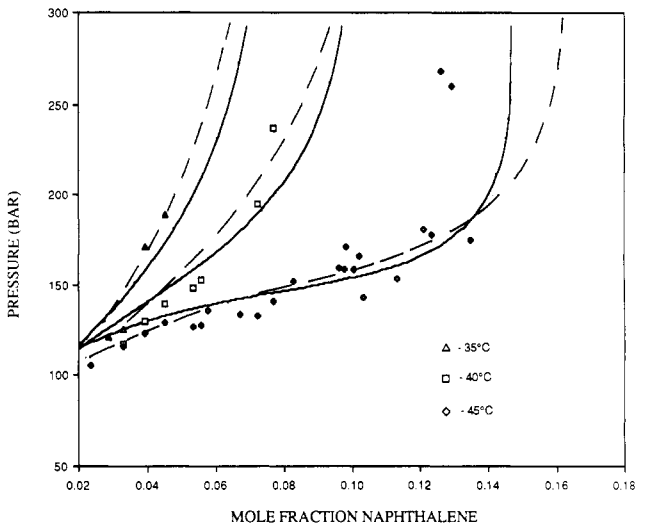

Figure 8. Comparison of calculated and experimental solid-solubility isotherms. The data of Krukonis et al. (1984) are included on this figure. The solid lines are calculations with the Peng–Robinson equation with k_{ij} equal to 0.020 and η_{ij} equal to −0.025. The dashed lines are calculations with the Sanchez–Lacombe equation with k_{ij} equal to 0.030 44 and η_{ij} equal to −0.0354.

were the results obtained with the Peng–Robinson equations. Figure 8 shows calculated solid-solubility isotherms using the mixture parameters found from the fit of the SLG line. At 35 and 40 °C, the fit with the Sanchez–Lacombe equation is slightly better than that obtained with the Peng–Robinson equation. At 45 °C, the fit of the data is very similar for both equations up to about 175 bar. At pressures above 175 bar, the solubilites calculated with the Sanchez–Lacombe equation are about 25% too high.

The calculated phase behavior in Figures 6–8 shows that a reasonable estimate for the phase behavior of a solid–gas system can be obtained with either the Peng–Robinson or the Sanchez–Lacombe equations of state, each with two mixture parameters fitted to the SLG line. The P–T trace of the SLG line is experimentally easier to obtain than solid-solubility and critical-mixture data, and it also defines the P–T boundaries where supercritical fluid extraction of a solid is possible. Hence, by fitting the mixture parameters in these equations to the "easier-to-obtain" data, it is possible to generate reasonable estimates for the solubility of a nonvolatile solid in a supercritical fluid as well as other features of the phase diagram such as the critical-mixture curve and the P–T conditions for phase inversions.

Both equations of state are easy to implement; however, they do differ in the amount of pure component information that is needed to determine the pure component parameters used in the equations. The Peng–Robinson equation uses critical property information, while the Sanchez–Lacombe equation uses vapor–liquid equilibrium data along with liquid molar–volume data. The Peng–Robinson equation is limited in use to low-to-moderate molecular weight species for which critical-property information is available. The Sanchez–Lacombe equation can be used to model the phase behavior of large molecular weight species, including polymers and, hence, has a greater utility for modeling the behavior of mixtures consisting of a low molecular weight gas and a large molecular weight nonvolatile substance (Kiszka et al., 1988). Although more work needs to be done with the Sanchez–Lacombe equation of state to correlate the mixture parameters, k_{ij} and η_{ij}, to the pure component properties of the mixture components, the results of this short study suggest that k_{ij} and η_{ij} should have values similar to those found with the Peng–Robinson equation.

Conclusions

In this paper we have shown the utility of using a more exacting technique for obtaining the P–T trace of the SLG line ending at the UCEP. We have added experimental information about the critical-mixture curve and solid-solubility isotherms for the xenon–naphthalene system. And we have shown how a simple equation of state, either the Peng–Robinson or the Sanchez–Lacombe, can be used with a small amount of experimental data to generate major portions of the P–I diagram, thus reducing the amount of experimental effort needed to understand the phase behavior for a particular solid–supercritical fluid system.

Although both the Peng–Robinson and the Sanchez–Lacombe equations represent the experimental data with about the same accuracy, each of these equations has different strengths. The Peng–Robinson equation uses the critical properties of the pure components which, for very large species, may not be available. The Sanchez–Lacombe equation does not need critical properties to determine pure component parameters but does need some VLE data and liquid molar volume data. The main advantage with the Sanchez–Lacombe equation is that is can be used for large molecule systems, including polymer–solvent mixtures, whereas the Peng–Robinson equation is limited to low-to-moderate molecular weight systems.

Acknowledgment

We thank the Exxon Education Foundation for partial support of this project and the BOAC Group who donated the xenon used in this study. We also thank Melchior Meilchen for helping with the calculations presented in this paper. Mark McHugh especially thanks Rahoma Mohamed, who pointed out the error in eq 5.17d in McHugh and Krukonis (1986).

Nomenclature

F = fugacity
k_{12} = mixture parameter
m_i = weight fraction of component i
P = pressure
$\tilde{P}$ = reduced pressure
r = number of lattice sites occupied by a molecule
R = gas constant
T = temperature
$\tilde{T}$ = reduced temperature
v = molar volume
$\tilde{v}$ = reduced volume
x = mole fraction
z = compressibility

Greek Symbols

ϵ = interaction energy
η_{ij} = mixture parameter
ρ = density
$\tilde{\rho}$ = reduced density
ϕ_i = close-packed volume fraction of component i; fugacity coefficient

Subscripts

C = critical property
i = component i
M2 = melting temperature of component 2
m,mix = mixture
Xe = xenon
1 = xenon
2 = naphthalene

Superscripts
F = fusion
G = gas
L = liquid
o = pure component
s = solid
sub = sublimation
* = characteristic variable

Appendix. Determination of Fugacity Coefficients Using the Sanchez-Lacombe Equation of State

By definition, the fugacity coefficient of a mixture is given as

$$\ln \phi_m = \int_V^\infty \left\{\frac{P}{RT} - \frac{1}{V}\right\} dV + Z - 1 - \ln Z \quad \text{(A1)}$$

where V is the total volume of the mixture and Z is the compressibility factor which, in terms of the Sanchez–Lacombe equation, is defined as

$$Z = \frac{r\tilde{P}\tilde{v}}{\tilde{T}} \quad \text{(A2)}$$

The natural log of the fugacity coefficient of the mixture is obtained by substituting the Sanchez–Lacombe equation of state into eq A1:

$$\ln \phi_m = \{\tilde{v} - 1\}r \ln\left\{1 - \frac{1}{\tilde{v}}\right\} - \frac{r}{\tilde{T}\tilde{v}} + r + Z - 1 - \ln Z \quad \text{(A3)}$$

Equation A3 is then substituted into eq 24. The following expression was derived for $\ln \phi_m$ by using the chain rule of differentiation,

$$\frac{\partial \ln \phi_m}{\partial x_1} = \frac{\partial \ln \phi_m}{\partial \tilde{v}}\frac{\partial \tilde{v}}{\partial x_1} + \frac{\partial \ln \phi_m}{\partial r}\frac{\partial r}{\partial x_1} + \frac{\partial \ln \phi_m}{\partial \tilde{T}}\frac{\partial \ln \phi_m}{\partial x_1} + \frac{\partial \ln \phi_m}{\partial Z}\frac{\partial Z}{\partial x_1} \quad \text{(A4)}$$

where the derivatives in eq A4 are

$$\frac{\partial \ln \phi_m}{\partial \tilde{v}} = \frac{r}{\tilde{v}} + r \ln\left\{1 - \frac{1}{\tilde{v}}\right\} + \frac{r}{\tilde{T}\tilde{v}^2} \quad \text{(A5)}$$

$$\frac{\partial \ln \phi_m}{\partial r} = \{\tilde{v} - 1\} \ln\left\{1 - \frac{1}{\tilde{v}}\right\} - \frac{1}{\tilde{T}\tilde{v}} + 1 \quad \text{(A6)}$$

$$\frac{\partial \ln \phi_m}{\partial \tilde{T}} = \frac{r}{\tilde{v}\tilde{T}^2} \quad \text{(A7)}$$

$$\frac{\partial \ln \phi_m}{\partial Z} = 1 - \frac{1}{Z} \quad \text{(A8)}$$

$$\frac{\partial \tilde{v}}{\partial x_1} = -\left\{\frac{\tilde{v}}{r}\right\}\left\{\frac{\partial r}{\partial x_1}\right\} - \left\{\frac{\tilde{v}}{v^*_{mix}}\right\}\left\{\frac{2\phi_1\phi_2}{x_1x_2}\right\} \times \{\phi_1 v_{11}^* - \phi_2 v_{22}^* + (\phi_2 - \phi_1)v_{12}^*\} + \left\{\frac{\tilde{v}}{x_1}\right\} \quad \text{(A9)}$$

$$\partial r/\partial x_1 = r_1^\circ - r_2^\circ \quad \text{(A10)}$$

$$\frac{\partial \tilde{T}}{\partial x_1} = \left\{-\frac{\tilde{T}}{\epsilon_{mix}v^*_{mix}}\right\}\left\{\frac{2\phi_1\phi_2}{x_1x_2}\right\}\{\phi_1 v_{11}^*(\epsilon_{11} - \epsilon_{mix}) - \phi_2 v_{22}^*(\epsilon_{22} - \epsilon_{mix}) + (\phi_2 - \phi_1)v_{12}^*(\epsilon_{12} - \epsilon_{mix})\} \quad \text{(A11)}$$

$$\frac{\partial \tilde{P}}{\partial x_1} = \left\{\frac{\tilde{P}}{\epsilon_{mix}v^*_{mix}}\right\}\left\{\frac{2\phi_1\phi_2}{x_1x_2}\right\}\{\phi_1 v_{11}^*(2\epsilon_{mix} - \epsilon_{11}) - \phi_2 v_{22}^*(2\epsilon_{mix} - \epsilon_{22}) + (\phi_2 - \phi_1)v_{12}^*(2\epsilon_{mix} - \epsilon_{12})\} \quad \text{(A12)}$$

$$\frac{\partial z}{\partial x_1} = \frac{\tilde{P}\tilde{v}}{\tilde{T}}\frac{\partial r}{\partial x_1} + \frac{r\tilde{v}}{\tilde{T}}\frac{\partial \tilde{P}}{\partial x_1} + \frac{r\tilde{P}}{\tilde{T}}\frac{\partial \tilde{v}}{\partial x_1} - \frac{r\tilde{P}\tilde{v}}{\tilde{T}^2}\frac{\partial \tilde{T}}{\partial x_1} \quad \text{(A13)}$$

Equations A3–A13 are substituted into eq 24 along with values for the pure component parameters for each component.

Registry No. Xe, 7440-63-3; naphthalene, 91-20-3.

Literature Cited

API Tables, Research Project 44, loosefleaf supplements to 1980; American Petroleum Institute and the Thermodynamics Research Center, Texas A&M University, College Station, TX.

Dieters, U.; Schneider, G. M. "Fluid Mixtures at High pressures: Computer Calculations of the Phase Equilibria and the Critical Phenomena in Fluid Binary Mixtures from the Redlich–Kwong Equation of State". *Ber. Bunsenges. Phys. Chem.* **1976**, *80*, 1316.

De Swaan Arons, J.; Diepen, G. A. M. "Thermodynamic Study of Melting Equilibria under Pressure of a Supercritical Gas". *Recl. Trav. Chim. Pays-Bas* **1963**, *82*, 249.

Everett, D. H.; Stageman, J. F. "Preparation and Stability of Novel Polymer Colloids in a Range of Simple Liquids". *Faraday Discuss. Chem. Soc.* **1978**, *65*, 230.

French, S. B.; Novotony, M. "Xenon, a Unique Mobile Phase for Supercritical Fluid Chromatography". *Anal. Chem.* **1986**, *58*, 164.

Kiszka, M. B.; Meilchen, M.; McHugh, M. A. "Modeling High-Pressure Gas–Polymer Mixtures Using the Sanchez–Lacombe Equation of State". *J. Appl. Polym. Sci.* **1988**, in press.

Krukonis, V. J.; McHugh, M. A.; Seckner, A. J. "Xenon as a Supercritical Solvent". *J. Phys. Chem.* **1984**, *88*, 2687.

Lacombe, R. H.; Sanchez, I. C. "Statistical Thermodynamics of Fluid Mixtures". *J. Phys. Chem.* **1976**, *80*, 2568.

Marshall, D. B.; Strohbusch, F.; Eyring, E. M. "Solubility of Organic Substances in Liquid Xenon". *J. Chem. Eng. Data* **1983**, *26*, 333.

McHugh, M. A.; Krukonis, V. J. *Supercritical Fluid Extraction: Principles and Practice*; Butterworth: Stoneham, MA, 1986; Chapter 3.

McHugh, M. A.; Yogan, T. J. "A Study of Three Phase Solid–Liquid–Gas Equilibria for Three Carbon Dioxide–Solid Hydrocarbon Systems, Two Ethane–Hydrocarbon Solid Systems and Two Ethylene–Hydrocarbon Solid Systems". *J. Chem. Eng. Data* **1984**, *29*, 112.

McHugh, M. A.; Seckner, A. J.; Yogan, T. J. "High-Pressure Phase Behavior of Octacosane and Carbon Dioxide". *Ind. Eng. Chem. Fundam.* **1984a**, *23*, 493.

McHugh, M. A.; Seckner, A. J.; Krukonis, V. J. "Supercritical Xenon". Presented at the AIChE Meeting, San Francisco, CA, Nov 1984b.

Michels, A.; Wassenaar, T.; Louwerse, P. "Isotherms of Xe". *Physica* **1954**, *20*, 99.

Occhiogrosso, R. N.; Igel, J. T.; McHugh, M. A. "The Phase Behavior of Isopropylbenzene–CO_2 Mixtures". *Fluid Phase Equilib.* **1986**, *26*, 1088.

Paulaitis, M. E.; McHugh, M. A.; Chai, C. P. "Solid Solubilities in Supercritical Fluids at Elevated Pressures". In *Chemical Engineering at Supercritical Fluid Conditions*; Paulaitis, M. E., Penninger, J. M. L., Gray, R. D., Davidson, P., Eds.; Ann Arbor Science: Ann Arbor, MI, 1983; p 139.

Peng, D.-Y.; Robinson, D. B. "A New Two Constant Equation of State". *Ind. Eng. Chem. Fundam.* **1976**, *15*, 59.

Rentzepis, P. M.; Douglas, D. C. "Xenon as a Solvent". *Nature (London)* **1981**, *293*, 165.

Russell, F. R.; Hottel, H. C. "Compressibility of Liquid Naphthalene". *Ind. Eng. Chem.* **1938**, *30*, 343.

Sanchez, I. C.; Lacombe, R. H. "Statistical Thermodynamics of Polymer Solutions". *Macromolecules* **1978**, *6*, 1145.

Smith, R. D.; Frye, S. L.; Yonker, C. R.; Gale, R. W. "Solvent Properties of Supercritical Xe and SF_6". *J. Phys. Chem.* **1987**, *91*, 3059.

Streett, W. E. "Phase Equilibria in Molecular Hydrogen–Helium Mixtures at High Pressure". *Astrophys. J.* **1973**, *186*, 1107.

Vaidya, S. N.; Kennedy, G. C. "Compressibility of 18 Molecular Organic Solids to 45 kbar". *J. Chem. Phys.* **1971**, *55*, 987.

van Gunst, C. A.; Scheffer, F. E. C.; Diepen, G. A. M. "On Critical Phenomena of Saturated Solutions in Binary Systems. II". *J. Phys. Chem.* **1953**, *57*, 578.

van Hest, J. A. M.; Diepen, G. A. M. "Solubility of Naphthalene in Supercritical Methane". *Symp. Soc. Chem. Ind. London* **1960**, 10.

van Welie, G. S. A.; Diepen, G. A. M. "The P–T–x Space Model of the System Ethylene–Naphthalene (I)". *Recl. Trav. Chim. Pays-Bas* **1961a**, *80*, 659.
van Welie, G. S. A.; Diepen, G. A. M. " P–T–x Space Model of the System Ethylene–Naphthalene (III)". *Recl. Trav. Chim. Pays-Bas* **1961b**, *80*, 673.
van Welie, G. S. A.; Diepen, G. A. M. "The Solubility of Naphthalene in Supercritical Ethane". *J. Phys. Chem.* **1963**, *67*, 755.
Vargaftik, N. B. *Handbook of Physical Properties of Liquids and Gases, Pure Substances and Mixtures*, 2nd ed.; Hemisphere: Washington, D.C., 1975; p 580.

Received for review September 17, 1987
Accepted January 27, 1988

Prediction of Solvent Activities in Polymer Solutions Using an Empirical Free Volume Correction

Michael J. Misovich and Eric A. Grulke*
Department of Chemical Engineering, Michigan State University, 173 Engineering Building, East Lansing, Michigan 48824-1226

A recent correlation for solvent activities in polymer solutions is extended in scope to provide a methodology for modeling nonideal effects in polymer solutions. This new method allows the use of any expression for the residual (enthalpic) interaction between polymer and solvent in conjunction with a standard (Flory–Huggins) expression for the combinatorial entropy. An empirical free volume correction uses the infinite dilution weight fraction activity coefficient of the solvent as an adjustable parameter. The new method is applied using one residual term given by the Analytical Solution of Groups (ASOG) technique, one similar to the Flory–Huggins interaction term, and one which yields no residual interaction. The results of these three models are compared to one another and to the Flory–Huggins model for 21 isothermal binary polymer–solvent systems. When adjustable parameters are determined by best fit to the data, each of the models applying the new method results in a standard error of less than 5% for at least 16 of the systems studied. This represented a better performance than the Flory–Huggins model.

An understanding of the thermodynamics of polymer solutions is important in practical applications such as polymerization, devolatilization, and the incorporation of plasticizers and other additives. Diffusion phenomena in polymer melts and solutions are strongly affected by nonideal solution behavior, since chemical potential rather than concentration provides the driving force for diffusion. Proper design and engineering of many polymer processes depend greatly upon accurate modeling of thermodynamic parameters such as solvent activities.

This work was an extension of previous work by the authors for correlating solvent activities in polymer solutions (Misovich et al., 1985). In that paper, an empirical free volume correction is derived from an athermal form of the Flory–Huggins combinatorial entropy (Flory, 1953), suggested by the Analytical Solution of Groups (ASOG) group-contribution model for calculation of activity coefficients in solution (Derr and Deal, 1969). The technique generally performs better than the classical Flory–Huggins equation in extrapolating solvent activity data from low solvent concentrations to higher concentrations. One deficiency of the approach is that phase separation cannot be predicted; i.e., $da_1/dw_1 > 0$ is always the case.

In this paper, the empirical free volume correction was modified to allow the explicit inclusion of an expression for residual (enthalpic) interaction between polymer and solvent. A general scheme was given to accomplish this, and three specific cases were analyzed and compared. One case used the ASOG expression for residual interaction, while a second used an interaction parameter approach similar to the Flory–Huggins equation. The third case assumed that there was no residual interaction term and reduced to the generalized correlation previously cited (Misovich et al., 1985).

The results in this paper were based upon a best fit of the adjustable parameters in each model using a least-squares evaluation of all the data, not by extrapolation from a single data point. In each of the three cases, the infinite dilution weight fraction solvent activity coefficient, Ω_1^∞, is an adjustable binary parameter. A residual interaction parameter is a second adjustable binary parameter in the second case. The classical Flory–Huggins equation was also fit to the data for comparison. In general, regardless of which residual interaction expression was used, the new method fits the data with less error than the Flory–Huggins equation.

Generalized Thermodynamic Modeling

Nonideal interactions between molecules in solution are generally classified in one of two categories. Interactions resulting from differences in the size or shape of molecules are classified as entropic, while interactions resulting from differences in energy are classified as enthalpic. The complete expression for solvent activity, a_1, is typically derived by multiplying concentration (mole fraction), x_1, a size or entropy activity coefficient, γ_1^S, and a enthalpy or group interaction activity coefficient, γ_1^G, or by adding their logarithms as shown in eq 1a. It is also common to lump the concentration with one of the activity coefficients (usually the entropic coefficient) to give eq 1b.

$$\ln a_1 = \ln x_1 + \ln \gamma_1^S + \ln \gamma_1^G \quad (1a)$$

$$\ln a_1 = \ln a_1^S + \ln \gamma_1^G \quad (1b)$$

A statistical approach allows entropic interactions to be handled combinatorially, as is done by the athermal Flory–Huggins equation (Flory, 1953), giving for the entropic contribution to activity, a_1^S

$$\ln a_1^S = \ln (x_1\gamma_1^S) = 1 - \phi_1 + \ln \phi_1 \quad (2)$$

where x_1 is the mole fraction, γ_1^S is the entropic activity coefficient, and ϕ_1 is the volume or segment fraction of component 1 (solvent). Staverman (1950) has also given an expression for combinatorial entropy which includes

0888-5885/88/2627-1033$01.50/0